SPIN
Vol. 2, No. 3 (2012) 1240002 (9 pages)

DOI: 10.1142/S2010324712400024

World Scientific
www.worldscientific.com

VOLTAGE-CONTROLLED MAGNETIC ANISOTROPY IN SPINTRONIC DEVICES

PEDRAM KHALILI AMIRI* and KANG L. WANG†
Department of Electrical Engineering
University of California, Los Angeles
CA 90095, USA
**pedramk@ucla.edu*
†*wang@ee.ucla.edu*

Received 20 July 2012
Accepted 6 September 2012
Published 29 October 2012

Electric-field-control of magnetism can dramatically improve the energy efficiency of spintronic devices and enhance the performance of magnetic memories. More generally, it expands the range of applications of nonvolatile spintronic devices, by making them energetically competitive compared to conventional semiconductor solutions for logic and computation, thereby potentially enabling a new generation of ultralow-power nonvolatile spintronic systems. This paper reviews recent experiments on the voltage-controlled magnetic anisotropy (VCMA) effect in thin magnetic films, and their device implications. The interfacial perpendicular anisotropy in layered magnetic material stacks, as well as its modulation by voltage, are discussed. Ferromagnetic resonance experiments and VCMA-induced high-frequency magnetization dynamics are reviewed. Finally, we discuss recent progress on voltage-induced switching of magnetic tunnel junction devices and its potential applications to magnetic random access memory (MRAM).

Keywords: Electric field; magnetoelectric effects; MRAM; spin transfer torque; nonvolatile memory.

1. Introduction

The field of spintronics emerged through the discovery of physical phenomena that allowed electrical currents and voltages to directly interact with magnetization in nanostructures, without the need for classical magnetic fields as intermediaries.[1–9] Starting with the discoveries of giant magnetoresistance (GMR)[8,9] and tunneling magnetoresistance (TMR),[3–7] which allowed electrical readout of the relative orientation of magnetic moments in spin valves and magnetic tunnel junctions (MTJs), spintronics was further advanced over the past decade following the theoretical prediction and experimental realization of the spin-transfer torque (STT) effect,[10–14] which allows the manipulation and switching of magnetization using electric currents. The STT effect has found numerous potential applications, most notably in magnetoresistive random access memory (STT−MRAM),[2,15–20] where writing is performed by passing currents directly through the MTJ memory bit, offering advantages in terms of energy efficiency, density and scalability over field-switched toggle MRAM. STT also offers applications in microwave devices such as oscillators.[12,14,21–29] When combined with CMOS logic circuitry, STT-based devices also offer the potential for the realization of nonvolatile logic

circuits[25,30–32] where standby power is eliminated and intermediate computation steps are stored in a nonvolatile manner, allowing for instant on/off capability.

Despite its significant potential impact as a nonvolatile candidate for replacing or complementing memory technologies such as dynamic and static random access memory (DRAM and SRAM), STT−MRAM still suffers from a shortcoming in terms of energy efficiency. This limitation on energy performance is brought about by the need for driving relatively large electrical charge currents through the device for switching, which, along with the nonzero voltage drop across the resistive MTJ, leads to significant power dissipation. The lowest switching energy of STT−MRAM devices is currently limited to ∼100 fJ,[16–18,33–37] which is still more than two orders of magnitude larger than modern CMOS transistors, which consume <1 fJ per switch. While this may not be a limitation for memory applications where energy efficiency is not the main concern or where frequent switching operations are not needed, it can be an important issue in applications where memory is to be closely integrated with logic, hence necessitating frequent read and write operations. Examples include memories for systems on a chip[17] and hybrid CMOS−MTJ nonvolatile logic circuits,[30–32,38,39] which are severely constrained by their energy consumption if STT-based write mechanisms are used for the memory.[30]

A number of proposals have been set forth in order to address this challenge. In this paper we will review efforts to use voltage (i.e., electric fields), rather than currents to control magnetization, which allow for much lower power dissipation since in principle, no charge flow is required in structures based on such voltage-controlled effects. Specifically, a number of recent experiments have targeted the study and realization of interfacial electric field controlled effects in MTJs similar to those used in STT devices. While only a subset of the entire body of work on voltage-control of magnetism, these experiments point to the possibility of using similar material structures and fabrication processes as those already developed for STT−MRAM, hence allowing for a faster technological adoption once viable devices have been developed.

The paper is organized as follows. Section 2 offers an introduction to the voltage-controlled magnetic anisotropy (VCMA) effect in magnetic nanostructures, which forms the basis for devices discussed in later sections. Recent experimental progress on perpendicular interface anisotropy in MTJs, and in particular its modulation by electric fields, will be discussed. Section 3 discusses microwave manifestations of the VCMA effect, as observed in ferromagnetic resonance (FMR) measurements. Section 4 reviews applications of the VCMA effect in memory devices, including voltage-assisted switching of MTJs, as well as spintronic charge-trap memory cells. Implications of using VCMA-based memory cells for MRAM are discussed in Sec. 5, emphasizing potential energy, density and scalability advantages over purely STT-based memory. This is followed by a summary and conclusions in Sec. 6.

2. VCMA in Thin Magnetic Films

Interfaces of magnetic films with nonmagnetic materials are magnetoelectric (ME), i.e., their magnetic properties exhibit a sensitivity to electric fields.[40–42] In particular, it has been demonstrated that the interface of oxides such as MgO with metallic ferromagnets such as Fe-rich CoFeB can exhibit a large perpendicular magnetic anisotropy (PMA),[20,33,37,43,44] which is furthermore sensitive to voltages applied across the dielectric layer,[40–42,45–54] an effect that has been attributed to spin-dependent charge screening and to the electric-field-induced modulation of the relative occupancy of d orbitals at the interface.[40–42,45] If MgO is used as the dielectric barrier, this voltage-controlled anisotropy effect can be incorporated into MTJ devices with high TMR ratios[4,5] for applications such as memory.

The PMA effect in a MgO/$Co_{20}Fe_{60}B_{20}$/Ta structure is illustrated in Fig. 1, where a gradual transition of the film magnetization from in-plane to out-of-plane is observed as the $Co_{20}Fe_{60}B_{20}$ layer thickness is reduced.[33] The inset in Fig. 1(b) shows the measured total perpendicular anisotropy as a function of film thickness, with a transition at ∼1.5 nm. Above this thickness, the shape-induced demagnetizing field (favoring in-plane magnetization) becomes larger than the interfacial anisotropy (favoring perpendicular magnetization). This interfacial PMA effect has been used to realize fully perpendicular MTJs,[37] to reduce switching current in in-plane MTJs,[33] and to increase output power and generation efficiency in spin torque nanooscillators.[29] Near the transition thickness, however, the magnetization configuration is most sensitive to

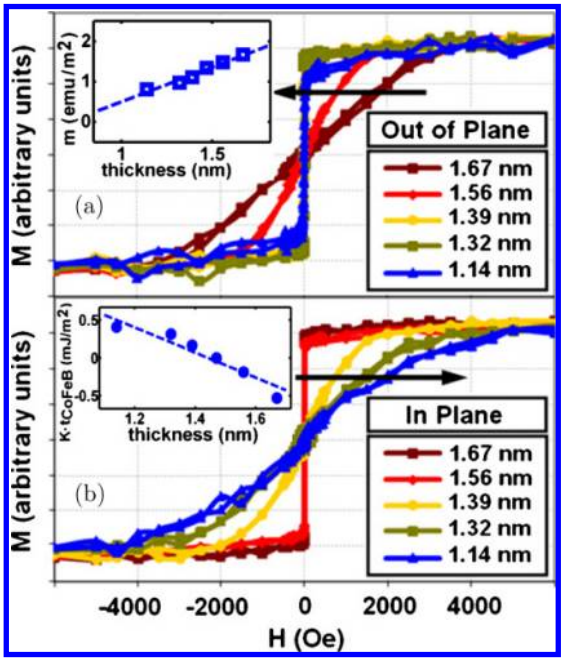

Fig. 1. Magnetization as a function of magnetic field, measured with (a) out-of-plane and (b) in-plane magnetic fields on films with varying $Co_{20}Fe_{60}B_{20}$ thicknesses, showing an increase of the interfacial PMA with decreasing film thickness. Inset in (a) shows the measured magnetic moment as a function of film thickness. Inset in (b) shows the dependence of total perpendicular anisotropy on film thickness, which is consistent with an interfacial origin of the perpendicular anisotropy and indicates a transition thickness of ∼1.5 nm. (Reprinted with permission from Ref. 33. Copyright 2011, American Institute of Physics.)

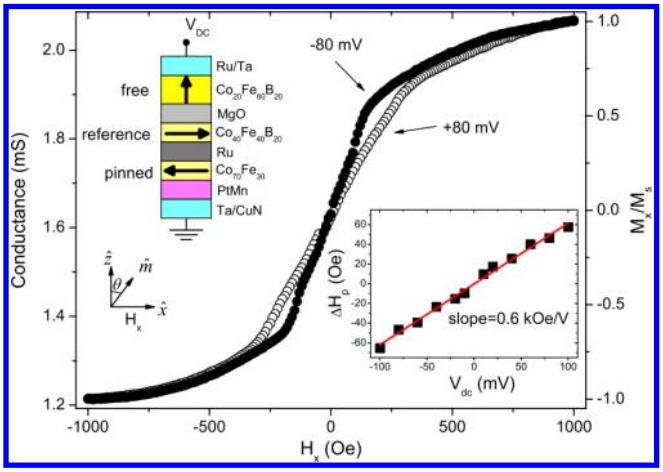

Fig. 2. Voltage-induced modulation of the perpendicular anisotropy in the free layer of a MTJ, observed by magnetoresistance measurements. The free layer is designed to have an out-of-plane magnetization, while the pinned layer is in-plane. The insets show the magnetic material stack and the dependence of the anisotropy on applied voltage. (Reprinted with permission from Ref. 46. Copyright 2012, American Physical Society.)

external voltages applied to the device,[55] and can therefore be used to realize electric-field-controlled MTJ devices.

The interfacial VCMA effect has been studied using a number of methods. A fairly straightforward approach to characterize its magnitude is to perform magnetometry measurements on a magnetic film as a function of applied electric field bias,[45] or (equivalently) to measure magnetoresistance curves of the device under different voltage bias conditions.[46] This approach has been used in Ref. 46, where values for the VCMA-induced anisotropy field modulation of ∼600 Oe/V have been obtained. Figure 2 illustrates the corresponding experiment described in Ref. 46. The pinned layer is in-plane in this experiment, while the $Co_{20}Fe_{60}B_{20}$ free layer thickness is designed such that its magnetization points out of plane, resulting in a nonhysteretic hard-axis behavior in the measured magnetoresistance loop when in-plane magnetic fields are applied. The slope of the curves in Fig. 2 corresponds to the PMA,[46] and is a function of the voltage bias applied to the device (compare curves for +80 mV and −80 mV bias).

In Ref. 47, a similar anisotropy modulation by electric fields is measured using the anomalous Hall effect. A $Co_{40}Fe_{40}B_{20}$ free layer composition is used, without the presence of a fixed layer, and both cases of in-plane and out-of-plane magnetization are studied. Magneto-optical Kerr effect (MOKE) measurements have been used in Ref. 50 to study the VCMA effect in $Co_{20}Fe_{80}$ films, also in the absence of a fixed layer. Another set of experiments have studied the VCMA effect in patterned MTJs using FMR techniques, with potential implications for radio-frequency (RF) devices.

3. VCMA-Induced FMR in Nanomagnets

The interfacial VCMA effect has been studied by microwave FMR measurements in a number of reports.[46,48,49,51] Early experiments demonstrated the static modulation of high-frequency magnetization dynamics using DC voltages. While the DC voltage in these studies led to an observable shift in the FMR[49] and spin wave[48] frequencies, the high-frequency dynamics themselves were not generated by electric fields. An example is shown in Fig. 3.[49] Here, current-induced magnetization dynamics were

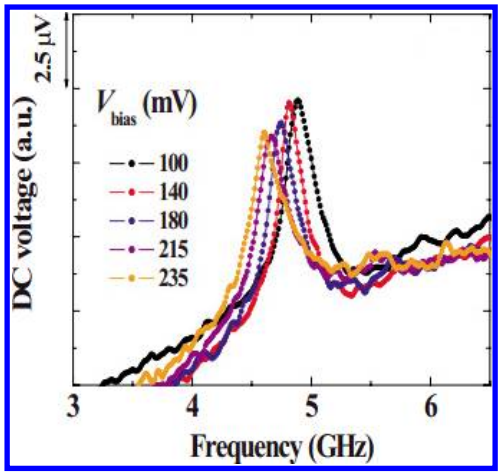

(a)

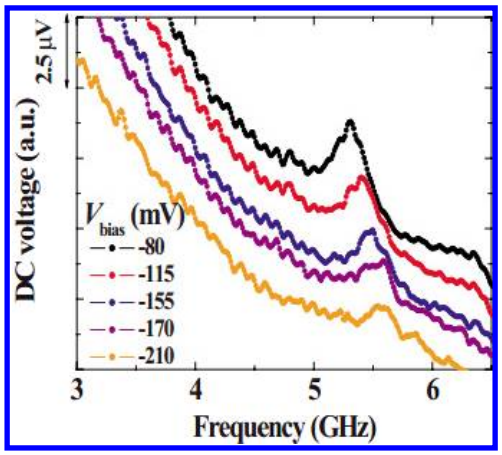

(b)

Fig. 3. Dependence of the FMR frequency in a MTJ on the DC voltage applied to it. FMR spectra are obtained by measuring the rectified voltage across the junction when a RF signal is applied to it. The additional DC bias voltage induces a change in the perpendicular anisotropy, thereby modulating the FMR frequency. (Reprinted with permission from Ref. 49. Copyright 2010, American Institute of Physics.)

generated by the STT effect in a low-resistance MTJ, using the rectified voltage across the MTJ to detect the FMR signature.[56,57] As can be seen in Fig. 3, the peak frequency of the FMR signal shifts as a function of the DC voltage applied across the MTJ, indicating an electric-field-induced modulation of the perpendicular anisotropy in the device.[49]

Similar to the case of MTJ switching, the use of currents (i.e., using STT, rather than voltages using VCMA) to induce high-frequency magnetization dynamics is energetically inefficient and leads to large Ohmic losses. This is a practical limitation in cases where RF dynamics need to be excited with high energy efficiency, such as in RF device applications,[21–23,56,58] as well as in potential future applications such as spin wave logic circuits.[59,60] Both for these practical reasons as well as for better fundamental understanding of the VCMA effect, the study of the RF electric-field-induced dynamics in magnetic nanostructures is of great interest. Recent works have addressed this in $Co_{20}Fe_{60}B_{20}$–MgO[46] and $Co_{20}Fe_{80}$–MgO[51] MTJs, where RF magnetization dynamics were directly generated through the application of a RF voltage to the device using the VCMA effect.

The experiment described in Ref. 46 is illustrated in Fig. 4. As in Fig. 2, the $Co_{20}Fe_{60}B_{20}$ free layer of the device is thin enough to point out of the sample plane, while the reference (pinned) layer is magnetized in-plane. The FMR signal is detected by measuring the rectified voltage across the device, when a RF voltage is applied to it, using a method similar to Refs. 49,51,56 and 57. Due to the relatively low resistance of the MTJs used in the experiment (with resistance–area product of 3.5 Ω-μm^2), both VCMA and STT effects are present when voltages are applied to the device and can be characterized separately by analysis of the resonance line shape.[46] Based on this, STT- and VCMA-induced torques were determined to have approximately equal magnitudes in this low-resistance

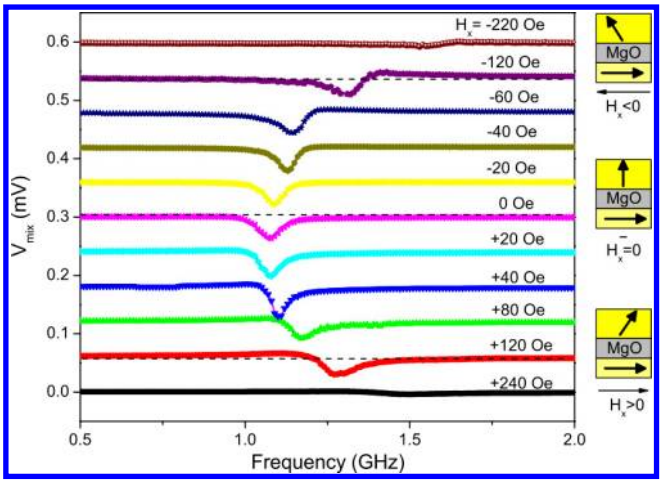

Fig. 4. VCMA-induced high-frequency magnetization dynamics in a MTJ. FMR spectra are obtained by measuring the rectified voltage across the junction when a RF signal is applied to it. Both STT and VCMA effects are present, and their relative contributions can be identified using the resonance line shape. (Reprinted with permission from Ref. 46. Copyright 2012, American Physical Society.)

junction, and furthermore the analysis in Ref. 46 shows that the magnitude of the VCMA effect at RF frequencies of a few GHz is comparable to that at DC, hence affecting the high-frequency (or short time-scale) behavior of the device. With increased device resistance, the relative contribution of the VCMA effect to the device behavior becomes larger compared to the current-induced STT effect.

Results such as those described in Refs. 46 and 51 demonstrate that the VCMA effect can be used directly to generate RF dynamics in high-resistance MTJs, where STT is suppressed due to small leakage currents, potentially conferring an advantage in terms of energy efficiency. As an example, Ref. 46 shows that the sensitivity of a MTJ microwave signal detector can be increased by ∼40%, reaching values close to those of Schottky diodes. Equally importantly, however, these results indicate the significant role played by VCMA even in regular current-controlled STT devices, such as low-resistance MTJ memory cells used for STT−MRAM. This is especially the case in STT−MRAM devices with large interfacial PMA, which are currently of increasing interest for reducing switching currents and increasing the scalability of STT−MRAM memory cells,[33,37] since materials used in these devices typically also exhibit large VCMA effects.

More specifically, however, the VCMA effect itself can also be used as the primary physical mechanism to bring about switching in magnetoelectric MRAM (i.e., MeRAM) memory cells that do not utilize the STT effect, i.e., which have resistances high enough to prevent the flow of large leakage currents, with potential advantages in terms of energy efficiency and density (due to smaller access transistor size) compared to STT−MRAM. The next section reviews some of the recent experiments on VCMA-induced switching of MTJs, for the realization of such a voltage-controlled nonvolatile magnetic memory.

4. VCMA Switching of MTJs

A number of recent works have demonstrated the feasibility of using VCMA to induce or assist in the switching of MTJs.[52,53,55] Compared to STT-induced switching, VCMA-induced switching offers the potential to reduce power dissipation and enhance density and scalability by eliminating the need for large drive currents, offering a pathway to applications beyond STT−MRAM where superior energy efficiency is required. Figure 5(a) illustrates a VCMA-controlled magnetic memory bit, with free and fixed layers as in a regular MTJ, allowing for the electrical readout of the memory state based on the TMR effect. Unlike STT−MRAM, however, the leakage current through the device is small, allowing for the applied voltage (electric field across the tunnel barrier) to control the switching behavior.

A possible switching mechanism in such a VCMA-based MTJ is illustrated in Fig. 6, assuming an in-plane magnetization in both free and fixed layers. The case of a fully perpendicular device follows similarly. Switching is realized through the modification of the interfacial perpendicular anisotropy when a voltage pulse is applied, i.e., by turning the free layer from a stable in-plane state to a meta-stable perpendicular state for a normally in-plane magnetized bit. Once the voltage pulse is removed, the free layer magnetization relaxes to one of the available in-plane states, with the final state being determined by the total magnetic field acting on the free layer. This total field is a combination of coupling fields from the fixed layer, as well as any external fields present in the experiment. Switching using this approach, therefore, requires a magnetic field to determine the switching direction, while voltages can be used to induce the switching using the VCMA effect.[55]

An example of switching results for such a voltage-assisted switching experiment is shown in Fig. 5(b).[53,55] While two different external magnetic fields (+60 Oe and −60 Oe) are used to bring about switching in this in-plane $Co_{20}Fe_{60}B_{20}$−MgO MTJ device, the switching itself is induced by VCMA, rather than STT, as evident from the large device resistance (i.e., leakage currents $<10\,\mu$A during switching). It is also worth noting that, unlike STT, both switching directions are realized using voltages of the same polarity in this experiment, further pointing to VCMA as the primary switching mechanism.[55] A switching experiment based on this principle for fully perpendicular MTJs is described in Ref. 53. Here, both magnetic electrodes consist of $Co_{40}Fe_{40}B_{20}$, and can each be switched using voltages of opposite polarities. The applied electric field pattern and measured resistance as a function of time are illustrated in Fig. 7.

The VCMA effect can also be used to bring about precessional switching of the magnetization in MTJs. This is qualitatively similar to current-induced precessional switching realized in STT−MRAM

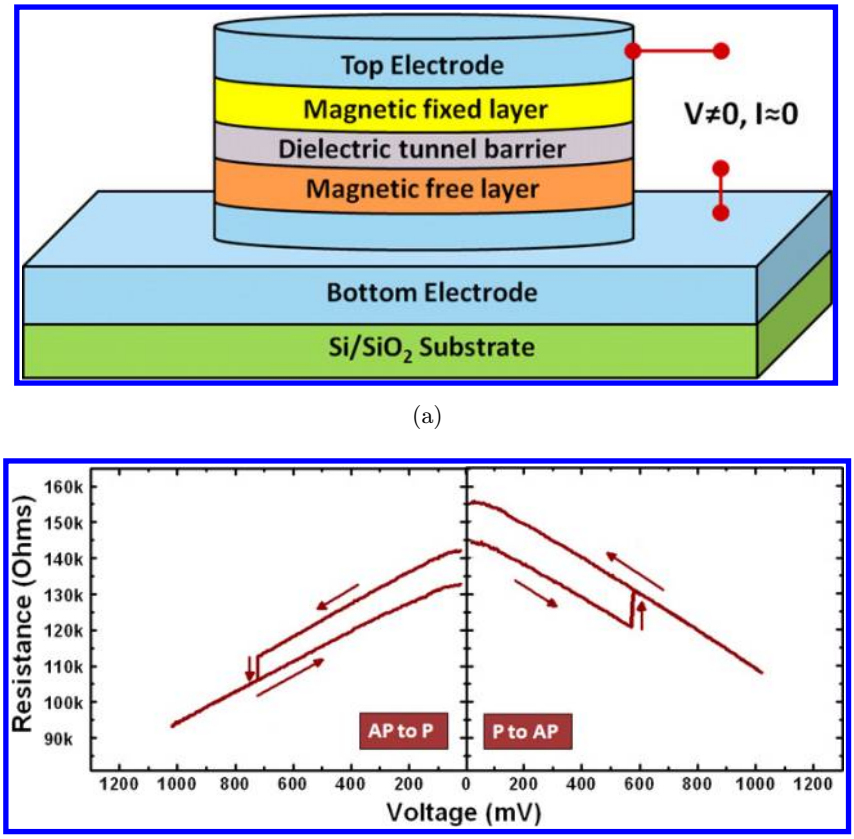

Fig. 5. Schematic illustration of a voltage-controlled MTJ (a) using the VCMA effect, where switching (b) of a magnetic free layer is achieved without the use of spin-polarized currents. Note that switching in both anti-parallel (AP, high-resistance) to parallel (P, low-resistance) and P to AP directions is performed with voltages of the same polarity, confirming the VCMA-induced switching mechanism.[55]

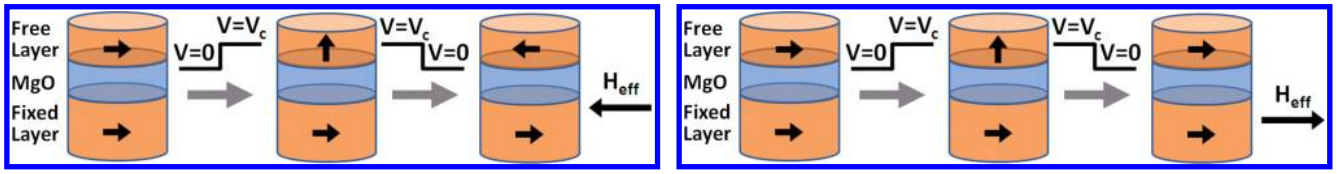

Fig. 6. Voltage-induced switching of an in-plane high-resistance MTJ. An applied voltage forces the magnetization into a metastable state, which then relaxes to a (similar or different) stable state after the voltage is removed.

devices,[35,36,61,62] with ultrafast switching times in the sub-500 ps range, but with potentially much better energy efficiency due to the purely electric-field-controlled effect. This type of switching is, however, sensitive to the precise width of the applied pulse, as illustrated in Fig. 8,[52] with the final state being determined by the number of precessions undergone by the free layer magnetization while the voltage is applied. Furthermore, as with the experiments described in Figs. 6 and 7, it does not provide direct voltage control over the direction of switching, instead only resulting in the free layer flipping to its opposite magnetic state upon application of each voltage pulse. Other effects (such as partial allowance for STT-induced dynamics) therefore need to be included in such VCMA-based MTJs in order to obtain the fully controllable bidirectional switching ideal for MRAM applications.

VCMA effects have also been incorporated into different types of non-MRAM devices. One example

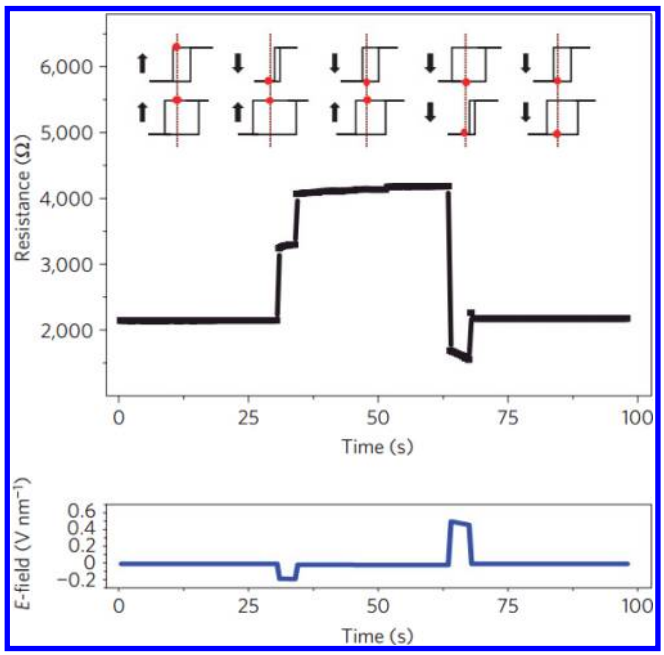

Fig. 7. Voltage-assisted switching of magnetization in a fully perpendicular MTJ. The switching is accomplished by modification of the free layer coercivity using an applied voltage, combined with the positioning of a DC bias magnetic field to accomplish switching. Top panel shows the measured resistance as a function of time, with the lower panel showing the applied electric field. (Reprinted with permission from Ref. 53. Copyright 2012, Macmillan Publishers Ltd: Nature Materials.)

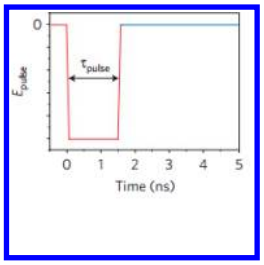

(a)

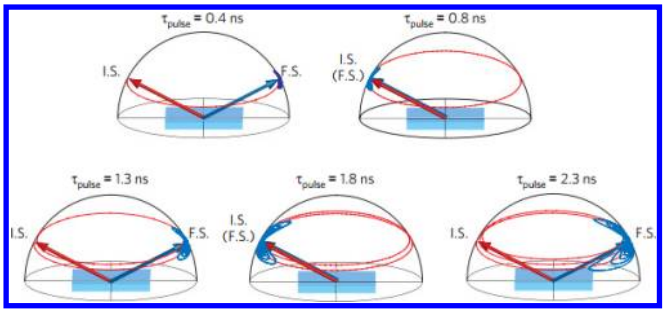

(b)

Fig. 8. Electric-field-induced precessional switching of magnetization in a MTJ. Figure shows macrospin simulations demonstrating the dependence of the final state on the applied voltage pulse width, i.e., on the number of precessions. Experimental data in Ref. 52 show a good agreement with simulations. (Reprinted with permission from Ref. 52. Copyright 2012, Macmillan Publishers Ltd: Nature Materials.)

is the voltage control of domain wall velocity in ultrathin magnetic films,[54] with potential applications to domain wall logic[63] and racetrack memory.[64] Another interesting example is a magnetoelectric charge trap memory,[65] where VCMA is used to provide a magnetic readout for a charge-based nonvolatile memory device. The device (see Fig. 9) contains a ZrO_2 charge-trap layer, where holes from an adjacent ITO electrode are trapped upon application of a voltage. Once the voltage is removed, the trapped charge creates an electric field across the MgO layer, affecting the perpendicular anisotropy of the thin Fe film beneath it. The device operates similar to a charge-trap Flash memory, except for the magnetic readout, which is allowed by the interfacial VCMA effect.

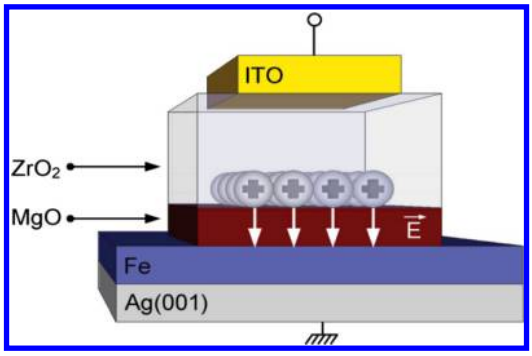

Fig. 9. Magnetoelectric charge-trap memory. An applied voltage pulse leads to the trapping of charges inside the dielectric layer of the device, which in turn exert an electric field on the Fe−MgO interface, changing its anisotropy. The charge-trap memory state can thus be read out by measuring the magnetic state of the Fe layer. (Reprinted with permission from Ref. 65. Copyright 2012, American Chemical Society.)

5. Implications for MRAM

STT−MRAM currently faces two challenges that could potentially limit both its ultimate scalability (hence density) and its range of applications beyond random access memory. Both originate from the fact that STT−MRAM relies on an entirely current-based write mechanism, where electric charge currents driven through a magnetic tunnel junction bit (by an access transistor) switch the magnetization of its free layer from one state to another.

The first challenge, as mentioned in the introduction, is the relatively high power dissipation associated with this current-controlled mechanism, which, while sufficiently low to be of interest for random access memory applications, may limit the usefulness of STT-based devices for applications beyond memory, such as nonvolatile logic.[30]

Second, in the typical 1-Transistor — 1-MTJ cell structure used for STT−MRAM,[16,17,19] the currents required to switch STT−MRAM bits require fairly wide transistors to drive them. This is in particular a problem for high-speed writing, since the switching current of STT−MRAM cells increases when the write pulse width is reduced. As a result, the density of STT−MRAM is in practice limited not by the dimensions of the memory bit (MTJ) itself, but rather by the switching current (i.e., access transistor size) required to write information into it. This problem gets increasingly more significant as one attempts to scale STT−MRAM to smaller bit dimensions while maintaining its nonvolatility.

While the development of new MTJ material structures with lower switching current densities — and in particular those based on perpendicularly magnetized free and fixed layers (see, e.g., Refs. 20 and 37) — is a quickly advancing area of research which could improve the scalability and energy efficiency of STT−MRAM, voltage-controlled VCMA-based memory cells could offer an alternative (or complementary) route towards a solution. VCMA-based memory development is therefore highly relevant for applications such as SRAM and DRAM replacement, as well as for hybrid CMOS−MTJ nonvolatile logic modules, where density, scalability, speed and/or power efficiency are important concerns.

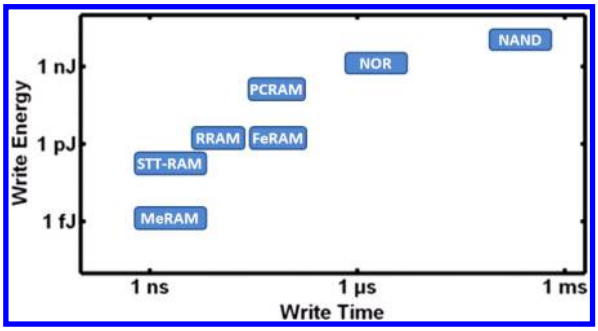

Fig. 10. Comparison of existing (NAND and NOR Flash) and emerging (MeRAM, STT−MRAM, Phase-Change, Ferroelectric and Resistive RAM) nonvolatile memory technologies in terms of energy dissipation and speed. MeRAM provides a significant improvement of energy efficiency, placing it in the preferred corner of the plot.

Figure 10 provides an illustration of the potential place of such a voltage-controlled magnetoelectric random access memory (MeRAM) on the nonvolatile memory landscape, comparing it to several existing and emerging technologies (see, e.g., Refs. 17 and 66) in terms of energy and speed. It is located in the preferred corner of the plot, potentially delivering speeds comparable to STT−MRAM while reducing the energy per bit by orders of magnitude.

6. Summary and Conclusions

The VCMA effect has generated a significant and growing interest in the magnetism community, with potential applications affecting many areas of spintronics research, including magnetic memory, microwave and domain wall devices. In the area of memory, VCMA may complement or even replace STT as the switching mechanism used in MRAM, with the potential to significantly enhance its energy efficiency. This will also affect other attributes of STT−MRAM such as density and scalability, through reducing (or eliminating) the need to pass currents through the memory bits for writing. By allowing for precessional switching, VCMA can also be used to realize ultrafast write times in magnetic memory cells. Successful realization of these advantages, however, will require development of improved material structures with larger VCMA effects (i.e., operation with lower voltages), while maintaining other important attributes such as high TMR for fast and low-power readout. For RF devices, VCMA has been shown in FMR measurements to affect the high-frequency dynamics of magnetization significantly, even in current-controlled devices with a significant STT effect. Further studies of VCMA at microwave frequencies may lead to both new device applications as well as to further insight into the VCMA effect itself. Finally, by providing a new mechanism for coupling the electrical and magnetic domains in nanostructures, VCMA can be expected to allow for novel spintronic device concepts and spark new directions for research in nanomagnetics.

References

1. S. A. Wolf *et al.*, *Science* **294**, 1488 (2001).
2. S. Ikeda *et al.*, *IEEE Trans. Electron Devices* **54**, 991 (2007).

3. M. Julliere, *Phys. Lett. A* **54**, 225 (1975).
4. S. S. P. Parkin *et al.*, *Nat. Mater.* **3**, 862 (2004).
5. S. Yuasa *et al.*, *Nat. Mater.* **3**, 868 (2004).
6. W. H. Butler *et al.*, *Phys. Rev. B* **63**, 054416 (2001).
7. J. Mathon and A. Umerski, *Phys. Rev. B* **63**, 220403 (2001).
8. G. Binasch *et al.*, *Phys. Rev. B* **39**, 4828 (1989).
9. M. N. Baibich *et al.*, *Phys. Rev. Lett.* **61**, 2472 (1988).
10. J. C. Slonczewski, *J. Magn. Magn. Mater.* **159**, L1 (1996).
11. L. Berger, *Phys. Rev. B* **54** 9353 (1996).
12. J. A. Katine *et al.*, *Phys. Rev. Lett.* **84**, 3149 (2000).
13. Y. M. Huai *et al.*, *Appl. Phys. Lett.* **84**, 3118 (2004).
14. M. Tsoi *et al.*, *Nature* **406**, 46 (2000).
15. Y. Huai, *AAPPS Bull.* **18**, 33 (2008).
16. E. Chen *et al.*, *IEEE Trans. Magn.* **46**, 1873 (2010).
17. K. Lee and S. H. Kang, *IEEE Trans. Magn.* **47**, 131 (2011).
18. P. K. Amiri *et al.*, *IEEE Electron Device Lett.* **32**, 57 (2011).
19. C. J. Lin *et al.*, 45 nm low power CMOS logic compatible embedded STT MRAM utilizing a reverse-connection IT/IMTJ cell, in *Electron Devices Meeting (IEDM), 2009 IEEE International*, 2009, pp. 1−4.
20. D. C. Worledge *et al.*, *Appl. Phys. Lett.* **98**, 022501 (2011).
21. S. I. Kiselev *et al.*, *Nature*, **425**, 380 (2003).
22. W. H. Rippard *et al.*, *Phys. Rev. Lett.* **92**, 027201 (2004).
23. Q. Mistral *et al.*, *Appl. Phys. Lett.* **88**, 192507 (2006).
24. J. A. Katine and E. E. Fullerton, *J. Magn. Magn. Mater.* **320**, 1217 (2008).
25. D. Houssameddine *et al.*, *Nat. Mater.* **6**, 447 (2007).
26. S. Kaka *et al.*, *Nature* **437**, 389 (2005).
27. F. B. Mancoff *et al.*, *Nature* **437**, 393 (2005).
28. V. S. Pribiag *et al.*, *Nat. Phys.* **3**, 498 (2007).
29. Z. Zeng *et al.*, *ACS Nano* **6**, 6115−6121 (2012).
30. F. B. Ren and D. Markovic, *IEEE Trans. Electron Devices* **57**, 1023 (2010).
31. S. Matsunaga *et al.*, *Appl. Phys. Exp.* **1**, 091301 (2008).
32. S. Matsunaga *et al.*, *Appl. Phys. Exp.* **2**, 023004 (2009).
33. P. K. Amiri *et al.*, *Appl. Phys. Lett.* **98**, 112507 (2011).
34. H. Zhao *et al.*, *J. Appl. Phys.* **109**, 07C720 (2011).
35. H. Liu *et al.*, *Appl. Phys. Lett.* **97**, 242510 (2010).
36. G. E. Rowlands *et al.*, *Appl. Phys. Lett.* **98**, 102509 (2011).
37. S. Ikeda *et al.*, *Nat. Mater.* **9**, 721 (2010).
38. S. Y. Lee *et al.*, *IEEE Trans. Electron Devices* **55**, 890 (2008).
39. H. Meng *et al.*, *IEEE Electron Device Lett.* **26**, 360 (2005).
40. J. P. Velev *et al.*, *Philos. Trans. R. Soc. A: Math. Phys. Eng. Sci.* **369**, 3069 (2011).
41. C.-G. Duan *et al.*, *Phys. Rev. Lett.* **101**, 137201 (2008).
42. C. G. Duan *et al.*, *Appl. Phys. Lett.* **92**, 122905 (2008).
43. S. Yakata *et al.*, *J. Appl. Phys.* **105**, 07D131 (2009).
44. W.-G. Wang *et al.*, *Appl. Phys. Lett.* **99**, 102502 (2011).
45. T. Maruyama *et al.*, *Nat. Nanotechnol.* **4**, 158 (2009).
46. J. Zhu *et al.*, *Phys. Rev. Lett.* **108**, 197203 (2012).
47. M. Endo *et al.*, *Appl. Phys. Lett.* **96**, 212503 (2010).
48. S. S. Ha *et al.*, *Appl. Phys. Lett.* **96**, 142512 (2010).
49. T. Nozaki *et al.*, *Appl. Phys. Lett.* **96**, 022506 (2010).
50. Y. Shiota *et al.*, *Appl. Phys. Exp.* **2**, 063001 (2009).
51. T. Nozaki *et al.*, *Nat. Phys.* **8**, 492 (2012).
52. Y. Shiota *et al.*, *Nat. Mater.* **11**, 39 (2012).
53. W.-G. Wang *et al.*, *Nat. Mater.* **11**, 64 (2012).
54. A. J. Schellekens *et al.*, *Nat. Commun.* **3**, 847 (2012).
55. J. G. Alzate *et al.*, Voltage-induced switching of CoFeB-MgO magnetic tunnel junctions, in *56th Conference on Magnetism and Magnetic Materials* Scottsdale, Arizona, 2011, pp. EG-11.
56. A. A. Tulapurkar *et al.*, *Nature* **438**, 339 (2005).
57. J. C. Sankey *et al.*, *Phys. Rev. Lett.* **96**, 227601 (2006).
58. X. Fan *et al.*, *Appl. Phys. Lett.* **95**, 122501 (2009).
59. A. Khitun *et al.*, *J. Phys. D-Appl. Phys.* **43**, 264005 (2010).
60. A. Khitun and K. L. Wang, *J. Appl. Phys.* **110**, 034306 (2011).
61. A. D. Kent *et al.*, *Appl. Phys. Lett.* **84**, 3897 (2004).
62. O. J. Lee *et al.*, *Appl. Phys. Lett.* **99**, 102507 (2011).
63. D. A. Allwood *et al.*, *Science* **309**, 1688 (2005).
64. S. S. P. Parkin *et al.*, *Science* **320**, 190 (2008).
65. U. Bauer *et al.*, *Nano Lett.* **12**, 1437 (2012).
66. M. H. Kryder and K. C. Soo, *IEEE Trans. Magn.* **45**, 3406 (2009).

This article has been cited by:

1. K L Wang, J G Alzate, P Khalili Amiri. 2013. Low-power non-volatile spintronic memory: STT-RAM and beyond. *Journal of Physics D: Applied Physics* **46**:7, 074003. [CrossRef]
2. P. Khalili Amiri, P. Upadhyaya, J. G. Alzate, K. L. Wang. 2013. Electric-field-induced thermally assisted switching of monodomain magnetic bits. *Journal of Applied Physics* **113**:1, 013912. [CrossRef]